Magazine of Civil Engineering. 2020. 93(1). Pp. 134–146
Инженерно-строительный журнал. 2020. № 1(93). С. 134–146

Magazine of Civil Engineering

ISSN 2071-0305

journal homepage: http://engstroy.spbstu.ru/

DOI: 10.18720/MCE.93.11

Impact behavior of rehabilitated post-tensioned slabs previously damaged by impact loading

***A. Jahami*[a]*, *Y. Temsah*[a], *J. Khatib*[b], *O. Baalbaki*[a], *M. Darwiche*[a], *S. Chaaban*[a]**
[a] *Beirut Arab University, Beirut, Lebanon*
[b] *University of Wolverhampton, Wolverhampton, UK*
** E–mail: ahjahamy@hotmail.com*

Keywords: rockfall, impact load, post-tension, shear reinforcement, energy, repair

Abstract. Accidental rockfalls are common hazards in many countries, where many structures and infrastructure are damaged by the impact of falling rocks. This research aims to study the efficiency of shear reinforcement as rehabilitation techniques for PT “post-tensioned” slabs damaged by falling rocks. Two simply supported PT slabs were considered in this study. Each has a dimension of (6.6 m×3 m×0.25 m) and was subjected to an impact from a 605 Kg reinforced concrete falling block at a height of 20 m. The first slab (PT-1) was hit at its center of gravity, while the second one (PT-2) was hit at the mid-span of its free edge. After impact, both slabs were repaired by replacing the damaged parts and adding shear ties in order to prevent any future collapse when new impact occurred. The impact test was repeated again after repairing, and both punching shear capacity and normal stresses were recorded. Results showed that the repaired slabs were able to resist the repeated impact successfully. Both punching shear and normal stress capacities were higher than the applied stresses. Moreover, using shear reinforcement helped in changing the crack pattern from shear to flexure. At the end of this study, some recommendations were suggested for further studies.

1. Introduction

Lebanon is characterized by its varied terrain (coast, mountains, and valleys). With the increase in population, people moved to live in the mountain region increasing the percentage of inhabitants there. Lebanon is also characterized by the heavy rain falling in the winter, causing incidents of landslides particularly in mountain areas resulting in rock falls onto the surfaces of residential buildings, leaving severe damage to the structure and threatening lives. This phenomenon is not limited in Lebanon but is a phenomenon that is spread throughout the world especially the mountain regions, which drew the attention of many researchers. The main issue related to this phenomenon is the impact caused by the rapid and sudden load application. Generally, most of the design codes do not include the impact load analysis -due to both falling objects and explosions- in analyses procedures; therefore, in the past ten years, numerous researches were conducted in this domain [1–6].

Iqbal [7] examined the behavior of post-tensioned slabs subjected to impact loading. Eight 800 mm×800 mm×100 mm (l×w×t) samples were considered in this study four of which were non-prestressed concrete samples and the others were prestressed at different stress levels. The impactor consisted of a 243 Kg steel mass dropped from two different heights 0.5 m and 1 m respectively. Results showed that post-tension slabs had a higher load capacity and a lower mid-span deflection compared to the non-prestressed concrete slabs. Yet, both types of slabs failed due to punching shear.

Al Rawi [8] studied numerically the effect of impact loads on prestressed concrete slabs compared to non-prestressed concrete slabs of equivalent moment capacity. Non-prestressed slabs gave better load capacity and deflection. In addition, Kumar [9] studied the efficiency of reinforced concrete slabs compared to

Jahami, A., Temsah, Y., Khatib, J., Baalbaki, O., Darwiche, M., Chaaban, S. Impact behavior of rehabilitated post-tensioned slabs previously damaged by impact loading. Magazine of Civil Engineering. 2020. 93(1). Pp. 134–146. DOI: 10.18720/MCE.93.11

Джахами А., Темсах Е., Хатиб Дж., Баалбаки О., Дарвич М., Чаабан С. Свойства восстановленных предварительно напряжённый плит, ранее поврежденных ударной нагрузкой // Инженерно-строительный журнал. 2020. № 1(93). С. 134–146. DOI: 10.18720/MCE.93.11

prestressed concrete slabs of the same thicknesses in absorbing impact energy. The study concluded that prestressed concrete slabs absorb more impact energy than reinforced concrete slabs causing less damage.

To strengthen RC elements to resist impact loads, there are many techniques that are used nowadays. A commonly used technique is fiber-reinforced polymers (FRP), and several researchers based their studies on it [10–12]. One of the important researches done in this field was conducted by Radnic [13]. It studied the behavior of two way reinforced concrete slabs strengthened with “carbon fiber reinforced polymer” (CFRP) sheets when subjected to impact loads. Eight samples of 100 cm×100 cm×5.5 cm dimensions were cast for experimental testing divided into two sets as follows: the first set consisted of four of normal samples and the second set was of four samples strengthened with CFRP sheets at the bottom surface. Three of each set of samples were subjected to an impact from different heights, and the fourth was subjected to a normal static test for comparison. When subjected to impact load, samples strengthened with CFRP gave a 10 % larger load capacity than the normal samples. This percentage increased to 25 % for the sample subjected to a static load. The low performance for CFRP in strengthening is due to the punching shear failure that occurred to all tested samples; which cannot be resisted by the CFRP sheets. This conclusion was confirmed by another study done by Jahami [14], where the behavior of post-tensioned slabs strengthened with CFRP sheets was compared numerically to post-tensioned slabs. A similar percentage difference in load capacity was reached. This proves how critical is the punching shear failure in impact loading and that CFRP is not ideal to resist impact loads.

Hao [15] investigated the effect of using steel fibers in concrete on the impact behavior of reinforced concrete beams. Three cases were considered in the study: the first was the control sample without fibers, the second one contained spiral steel fibers, and the third one contained hooked-end steel fibers. Each sample was subjected to a repeated impact from a 15.2 Kg mass dropped from a height of 5 meters. Results showed that spiral steel fibers are better in absorbing the impact energy and enhancing the structural performance for RC beams under impact loading. Some researchers studied the efficiency of different types of fibers in punching shear resistance. Harajli [16] did a comparative study between steel fibers and polypropylene fibers to determine which of them serves better in punching shear resistance. The results showed that both types increased the punching shear capacity in a significant way and in a similar ratio. In addition, the failure observed for both fibers was a ductile failure and more energy was dissipated compared to normal concrete. Furthermore, Mostafaei [17] studied the effect of external prestressing on punching shear behavior of SFRC “steel fiber reinforced concrete” slabs. Results showed that using external prestressing helped in increasing punching shear capacity significantly. Also, the combination of steel fiber and prestressing helped in improving the ductility and energy dissipation of slabs.

In conclusion, the effect of impact loads on reinforced concrete slabs has been extensively investigated. However, very few researchers have studied the behavior of post-tensioned slabs under impact load and the optimum repair techniques. This research aimed to study the rehabilitation of post-tensioned slabs previously damaged by the impact falling objects; which simulated the case of falling rocks in mountainous areas. As for non-mountainous areas, other types of impact may occur such as blast impact. These impacts may be considered in future research. In this study, two drop cases were considered; a drop at the center of gravity of the slab and a drop at the mid-span of the slab free edge. The following parameters were considered in this study; punching shear capacity, flexural normal stresses, slab vibration, slab damping ratio, damage mode, and the extent of damage.

2. Methods

2.1. Slabs preparation

Two PT “post-tensioned” slabs are considered in this study each having a 660 cm×300 cm×25 cm dimensions. The slabs are prestressed with six equally distributed mono strands and reinforced with-10mm diameter bottom and top mesh at 250 mm spacing (Figures 1 and 2). The prestressing mono-strands have a draped profile and are grouted after casting the concrete to form a bonded system. Slabs’ dimensions and reinforcements considered the different gravity loads that act on a residential floor. The supporting system consisted of 10 cm diameter steel cylinders of 12 cm height resting on steel I-shaped beams, and the whole system is supported on two (60 cm×60 cm) concrete strip footings (Figure 3). As for the falling mass used to hit the slabs, a 605 Kg reinforced concrete block (60 cm×60 cm×60 cm) is cast inside an 8mm thickness steel mold to protect the concrete core from severe damage after impact; to be used for multiple drops (Figure 4).

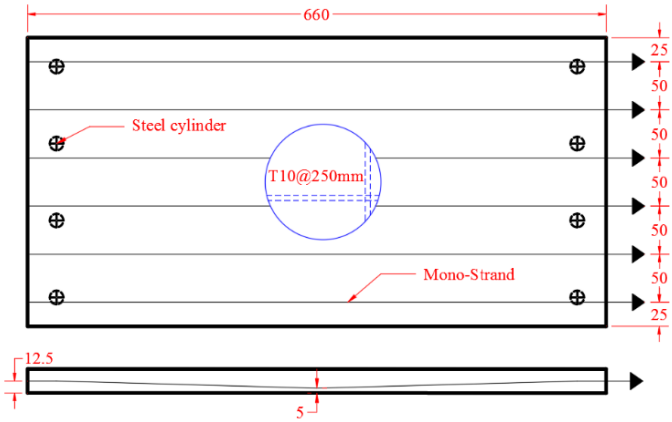

Figure 1. PT slab reinforcement (cm).

Figure 2. PT slab execution.

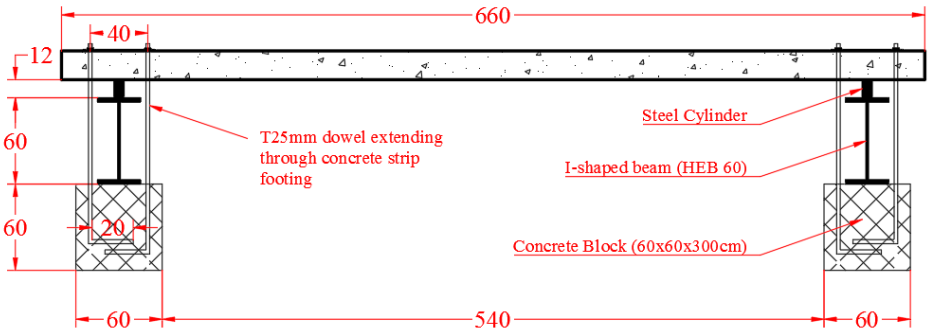

Figure 3. Slab supporting system (cm).

Figure 4. RC block reinforcement (cm).

The compressive strength test was conducted on three 15 cm diameter and 30 cm height cylinders specimens taken from the concrete batch after 28 days. The actual compressive strength of concrete is 32 MPa. The reinforcing steel rebars have yield and ultimate strengths of 585 MPa and 662 MPa respectively, and prestressed cables have yield and ultimate strengths of 1680 MPa and 1860 MPa respectively.

The experimental setup was prepared on different stages. During the First stage, all the timber formwork for the strip footings was set at a depth of 40 cm underground and the steel supporting system was prepared. Couples of 25 mm diameter steel dowels were added between the supports and extended to the concrete strip footings (Figure 3); in order to prevent the uplifting of slabs during impact. The footings then were cast and cured by water for about 7 days. After that, the I-shaped beams were placed over the strip footings and the steel cylinders were attached to them by bolts. Each cylinder had two 8 mm diameter and 15 cm length rebar welded to it and embedded inside the PT slab to form a pin support condition (Figure 5).

In the second stage, the slab formworks were prepared and the non-prestressed reinforcement was placed taking into consideration a clear cover of 2 cm. Then mono strands were placed as detailed in Figure 1, and special bursting steel was placed at the boundaries. After that concrete was cast and cured for two weeks with water, and mono-strands were stressed at 1400 MPa and grouted. Finally, a (150 cm×150 cm) neoprene pad was placed at the impact zone to redistribute pressure after hitting the slab with the falling block. One slab was hit at the center and named “PT-1”, and the other was hit at the free edge of the mid-span and named “PT-2” as shown in Figure 6.

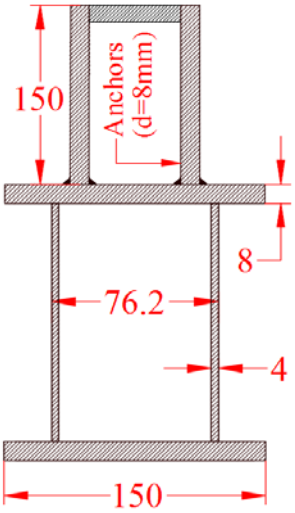

Figure 5. Steel cylinders (mm).

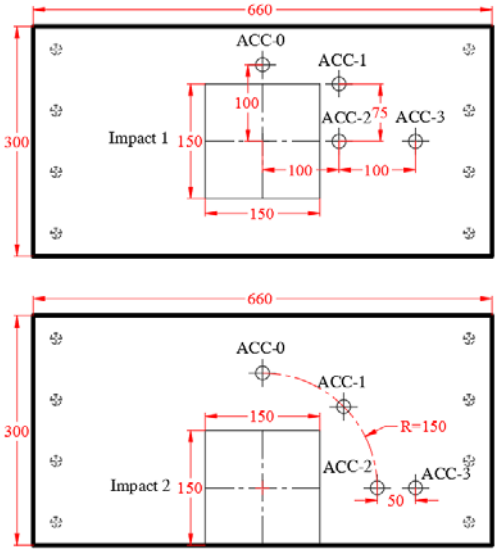

Figure 6. Impact position (cm).

In order to record the impact force and the slab displacement, the piezoelectric accelerometer sensors were used in this study. This type of sensors is adequate in the case of impact load; since it can record a large number of readings in a very short time. These sensors were used by much previous research [18, 19]. Four accelerometers were placed in each slab (PT-1 and PT-2) as illustrated in Figure 6. The position of each accelerometer was chosen such that it covers the critical slab zones. The data acquisition system used in this experiment consisted of: a (cDAQ-9178) with eight channels and a measurement card (NI 9234) which were provided by National Instrument [20]

On the testing day, a crane used to hold the 605 Kg RC block at a height of 20 m, where the total provided energy for the slabs was estimated based on the following equation:

$$E = mgh \tag{1}$$

Where E is the total provided energy for the system in (J), m is the mass of the falling object in (Kg), g is the gravitational acceleration and equal to (9.81 m/s^2), and h is the height of the falling object (m). In this case, the total provided energy was 118.7 KJ. The block height and position were specified exactly using a theodolite device. Each slab was hit once and different data were recorded including Impact load, mid-span displacement, type of damages and their extent in the different slabs. Results showed that the impact load was 1217 KN for slab PT-1 and 965 KN for slab PT-2. These values will be used to repair the slabs in the rehabilitation process.

2.2. Rehabilitation process

After the impact test, slabs were repaired so it can withstand another future impact. The proposed method was using shear reinforcement as a strengthening technique; since the mode of failure for slabs subjected to impact loading is punching shear. First, the damaged parts were removed. Removal area was determined based on punching shear analysis; where shear reinforcement distributed area must continue to reach a limit where concrete can alone resist the applied shear stress. Equation 2 shows the concrete two-way shear strength, whereas equation 4 shows the shear stresses carried by shear reinforcement [21]:

$$\upsilon_{con} = ((\beta_p \sqrt{f'c} + 0.3 f_{pc}) + \upsilon_p \quad (2)$$

$$\beta_p = \min(3.5, (\alpha_s d / b_0 + 1.5)) \quad (3)$$

$$v_s = \frac{A_{v.} f_y}{b.s} \quad (4)$$

Where v_{con} is the punching shear capacity of concrete, β_p is the factor used to compute v_{con} in pre-stressed concrete slab, f_y is the rebar yield strength. f'_c is the concrete compressive strength, f_{pc} is the average pre-compression stress in the critical section, υ_p is the vertical component of all effective pre-stress stresses crossing the critical section, v_s is the shear stress carried by shear reinforcement and it is the difference between the applied shear stress v_a and v_{con}, A_v is the total area of rebar legs at the critical section, b is the perimeter of the critical section, and s is the spacing of shear reinforcement and must be less than (d/2), where d is the effective depth of the section.

Therefore, for the PT slab subjected to an impact at its center of gravity "PT-1", the removal area was (2 m×3 m). Whereas for the slab subjected to an impact at the mid-span of its free edge "PT-2", the removal area was (4.8m x 3m). Figure 7 shows the removed area for slabs "PT-1" and "PT-2". The new slabs were named "PT-1R" for the rehabilitated "PT-1" slab and "PT-2R" for the rehabilitated "PT-2" slab. ACI code recommends reducing the concrete shear strength when using shear reinforcement to $\frac{1}{6}\sqrt{f_c}$. For more details regarding punching shear analysis and design, check Table 1:

Table 1. Punching shear calculation details for rehabilitated samples "PT-1R" and PT-2R".

Sample	V_a	d	b	s	f'_c	f_y	v_a	v_{con}	v_s
	(N)	(mm)	(mm)	(mm)	(MPa)	(MPa)	(MPa)	(MPa)	(MPa)
PT-1R	1216685	220	2880	100	31	585	1.92	0.93	0.99
PT-2R	964716	220	1940	100	31	585	2.26	0.93	1.33

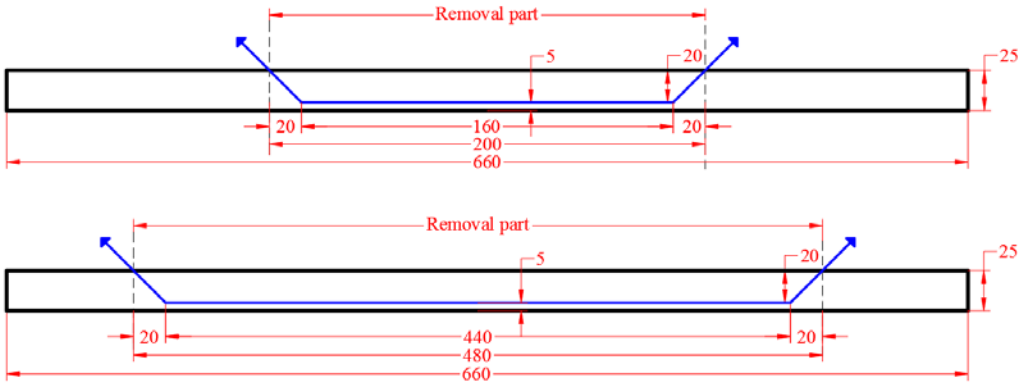

Figure 7. Removal area for both PT-1R and PT-2R & added mono-strands (cm).

Once the damaged zone is removed, all severely damaged non-prestressed reinforcement were replaced with new ones. A set of 10 mm diameter cross ties (punching shear reinforcement) was prepared – (Figure 8) – and attached to both top and bottom flexural reinforcement at a spacing of 10cm to cover the whole zone. As for the prestressing steel, all ducts were removed so strands are working as non-prestressed steel; since no bond remains between strands and concrete. Hence, and to regain the prestressing behavior in this zone, new mono strands were installed beside the old ones (Figure 9). The original flexural strength for both slabs before the first impact was 107.5 KN.m, whereas, after rehabilitation, the flexural strength increased to 118.6 KN.m. In order to achieve a better connection between the old and new concrete, an inclination of 45 degrees was performed in the interface. This interface was roughened to increase the friction between old and new concrete. Figure 10 shows slab PT-1R after finishing rehabilitation procedure before casting.

Finally, the new concrete was cast and cured with water for 2 weeks (Figure 11). Concrete mix strength was prepared to be the same as the old concrete cast for the first time. Three cylinders were tested at the impact test day and showed a compressive strength of 31 MPa. After casting, new sheets of neoprene pads were fixed at the impact zone as done previously, and accelerometers were placed at the same previous locations to have a valid comparison of the results with those of the original slabs before rehabilitation.

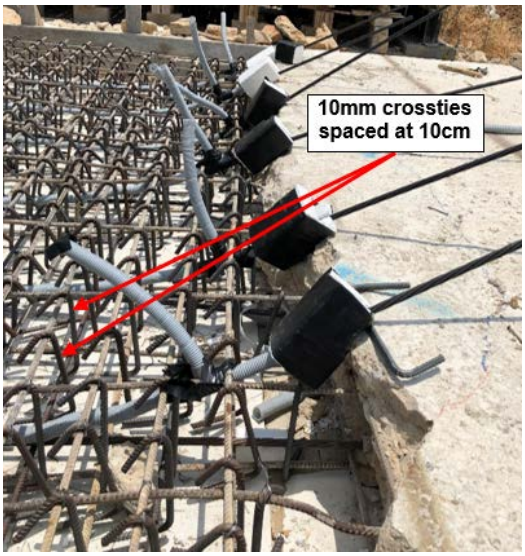

Figure 8. Crossties used in rehabilitation as punching shear reinforcement.

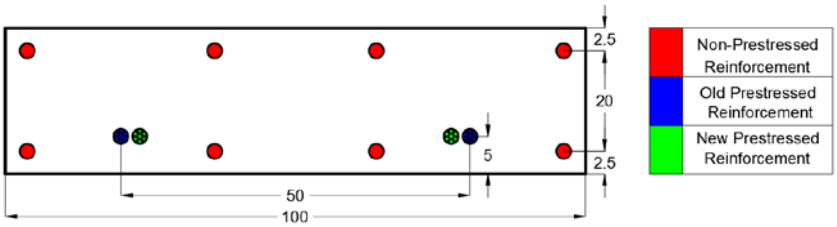

Figure 9. Flexural reinforcements detailing.

Figure 10. PT-1R slab before the concrete cast.

Figure 11. Concrete cast for PT-1R.

3. Results and Discussion

3.1. Impact load analysis

Table 2 summarizes the results of the impact testing for PT slabs before and after repair. Although the mass and height of the drop were maintained the same, the impact load was increased after repair regardless of the location of the dropped mass. This increase is 44 % and 71 % when the mass is dropped at the center (PT-1 and PT-1R) and at the edge (PT-2 and PT-2R) respectively. This is due to the position of the block at the moment it hits the slab. The block in case (PT-1) fell approximately at its flat surface, whereas for case (PT-1R) it fell at one of its edges as illustrated in the blue hatched zone in Figure 12. In addition, the block in case (PT-1) fell approximately at the center of the slab, while in case (PT-1R) it landed slightly to the right side of the neoprene pad limit (Figure 12). Therefore, accelerometer “ACC-2” which was closer to the drop position for slab PT-1R recorded a larger acceleration value than slab PT-1. As for cases (PT-2 and PT-2R), the block fell nearly in the same position in both cases. But in case (PT-2R) the block fell at one of its edges as shown in Figure 13 (blue hatch), while it fell on its flat surface for case (PT-2). Hence, accelerometer “ACC-0” that lies behind the hitting block edge for slab PT-2R recorded a larger acceleration value than slab PT-2.

Another important finding is the dynamic increase factor (DIF) for the impact test, which is the ratio between the static load (weight of block) and the equivalent load due to impact. For the impact energy of

118.7 KJ, the static weight for the falling object was magnified by 206.3, 296.8, 163.6, and 280 times for slabs PT-1, PT-1R, PT-2, and PT-2R respectively. This difference in the DIF factor is due to the variation in impact loads described earlier. This increase factor (DIF) is very important to be determined for any future analysis and design procedure.

Table 2. Applied load and punching shear analysis.

Slab	Static load (KN)	Impact load (KN)	Dynamic impact factor (DIF)	Applied punching shear stress v_a (MPa)	Punching shear capacity v_c (MPa)	Shear demand ratio (v_a/v_c)
PT-1	5.9	1217	206.3	1.92	1.83	1.05
PT-1R	5.9	1751	296.8	2.76	4.08	0.67
PT-2	5.9	965	163.6	2.26	1.83	1.23
PT-2R	5.9	1652	280	3.87	4.44	0.87

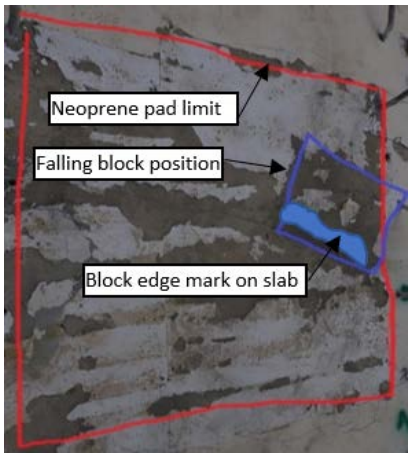

Figure 12. Position of the falling block on collision with slab PT-1R

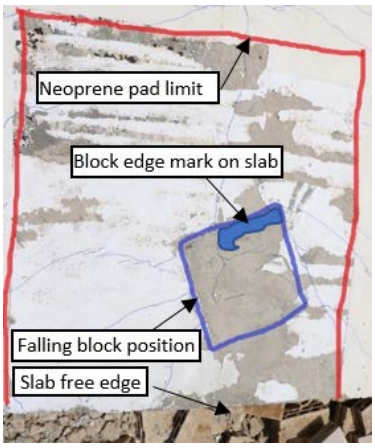

Figure 13. Position of the falling block on collision with slab PT-2R

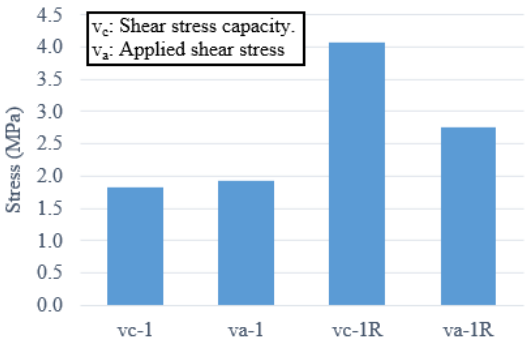

Figure 14. Shear stress for slabs PT-1 and PT-1R

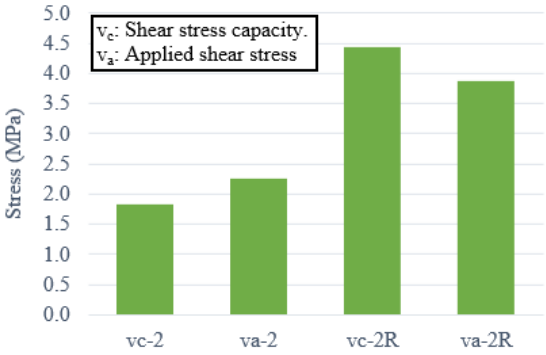

Figure 15. Shear stress for slabs PT-2 and PT-2R

Figure 14 shows the shear stress capacity and the applied shear stress for both slabs PT-1 and PT-1R. An increase of the punching shear capacity was observed from 1.83 MPa for slab PT-1 (before repair) to 4.08 MPa for slab PT-1R (after repair). This leads to a reduction in the shear demand ratio (v_n/v_{nc}) from 1.05 for slab PT-1 to 0.67 for slab PT-1R. As for slabs PT-2 and PT-2R, similar improvement was recorded where the shear capacity was increased from 1.83 MPa to 4.44 MPa respectively (Figure 15). This improvement was better for slab PT-2R than slab PT-1R; since the critical perimeter b for the edge drop case (PT-2R) is less than the critical perimeter for the center drop case (PT-1R), which led to a higher shear stress carried by crossties v_s in slab (PT-2R) than slab (PT-1R).

In order to prove the efficiency of the rehabilitation technique, a comparative study is conducted in order to prove the efficiency of the repair technique of slabs PT-1R and PT-2R in terms of flexural normal stresses. To achieve this goal, the outputs of the numerical analysis obtained in a previous investigation conducted by the authors were used to assess the flexure mode of failure [8]. Two main parameters were studied: the tensile stress at the bottom non-prestressed rebars and the compressive stress at the concrete top surface. Both parameters were studied using the dynamic properties of both concrete and steel rebars and not the static properties. The dynamic properties were examined using the CEB-FIP Model Code [22] that relates the dynamic to static properties for both steel and concrete based on strain rate. The dynamic yield strength of

non-prestressed rebars was 720 MPa compared to 585 MPa for static strength, while the dynamic compressive strength of concrete was 47 compared to a static strength of 32 MPa.

Figure 16 plots the axial tensile stress at steel rebars f_s below the impact zone. It can be noted that the non-prestressed rebars at slabs PT-1 and PT-1R reached a tensile stress value of 542 MPa and 452 MPa respectively, which is around 75 % and 63 % of the dynamic yield stress (720 MPa) of reinforcing rebars. On the other hand, rebars in slab PT-2 were yielded as shown in Figure 16, whereas slab PT-2R recorded a rebar tensile stress of 653 MPa, which is around 91 % of the dynamic yield stress. This suggests that both repaired slabs (PT-1R and PT-2R) did not experience any yielding in steel rebars.

The second parameter was represented in Figure 17, where the compressive stresses in concrete f_c at the top fibre of the slabs are shown in the impact zone. As per ACI318-14 [21] requirements, the stress in compression should not exceed 0.85f'c (i.e. 40 MPa) to avoid failure of concrete in compression. Results show that top compressive stresses for slabs PT-1 and PT-2 were 36 MPa and 41 MPa respectively, which means that slab PT-2 failed in compression. However, there was no compressive failure for both slabs after repairing, where the compressive stress was 30 MPa and 34 MPa for slabs PT-1R and PT-2R respectively. It was realized that for both top and bottom stresses slab PT-2R had higher values than slab PT-1R; because for slab PT-2R, the slab is hit at the mid-span of its free edge, which will lead to a higher top and bottom strain.

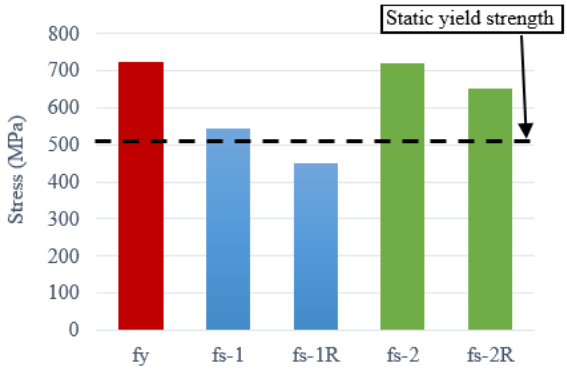

Figure 16. Rebar tensile stresses for slabs (PT-1, PT-1R, PT-2, and PT-2R)

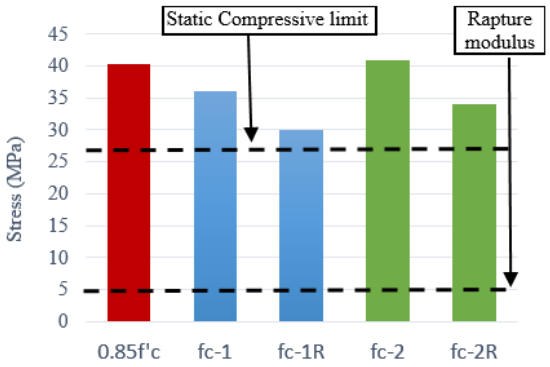

Figure 17. Top compression stresses for slabs (PT-1, PT-1R, PT-2, and PT-2R)

3.2. Vibration analysis

The displacement at each accelerometer was recorded using the double integration method for the acceleration curves. Table 3 summarizes the maximum displacement values for each accelerometer. For slab PT-1, the maximum displacement was recorded at ACC0 with a value of 40.4 mm. However, for slab PT-1R the maximum displacement was recorded at ACC2 (52.7 mm). This is due to the position of the block on collision where the edge of the block touched the slab first near ACC2. Compared to the displacement values at slab PT-1, the values recorded for slab PT-1R were higher; since the impact load was higher. A similar trend was realized for slabs PT-2 and PT-2R, where the maximum displacement was recorded at ACC2 (38.1 mm) for slab PT-2 and ACC0 (42 mm) for slab PT-2R. The higher displacement values for the repaired slab PT-2R is due to the higher impact load because of the position of the falling block. ACC1 results were not included since there were cracks across the accelerometers during impact.

One of the indicators that shows the efficiency of the repair technique is the “impact force to maximum displacement” (F/D) ratio, which is introduced for each accelerometer in Table 3. This ratio shows the force needed for each slab to generate a unit displacement. It can be clearly noticed that slab PT-1R performed better than slab PT-1 since it has a higher (F/D) ratio at all points (except ACC2). Results also showed an increase in the (F/D) ratio for slab PT-2R compared to slab PT-2. Moreover, it can be noticed that repairing techniques has more efficiency for the edge drop (PT-2 and PT-2R) than the central drop (PT-1 and PT-1R) in terms of (F/D) ratio. For more details, Figures 18 and 19 show the full displacement – time curves for slabs (PT-1 and PT-1R) and (PT-2 and PT-2R).

Table 3. Displacement results at each accelerometer.

Slab	ACC0 (mm)	ACC1 (mm)	ACC2 (mm)	ACC3 (mm)	$(F/D)_0$ (KN/mm)	$(F/D)_1$ (KN/mm)	$(F/D)_2$ (KN/mm)	$(F/D)_3$ (KN/mm)
PT-1	40.4	37.0	35.7	22.9	30.1	32.9	34.1	53.1
PT-1R	45.0	43.5	52.7	29.3	38.9	40.3	33.2	59.8
PT-2	35.4	--	38.1	27.8	27.3	--	25.3	34.8
PT-2R	42.0	--	40.0	35.0	39.3	--	41.3	47.2

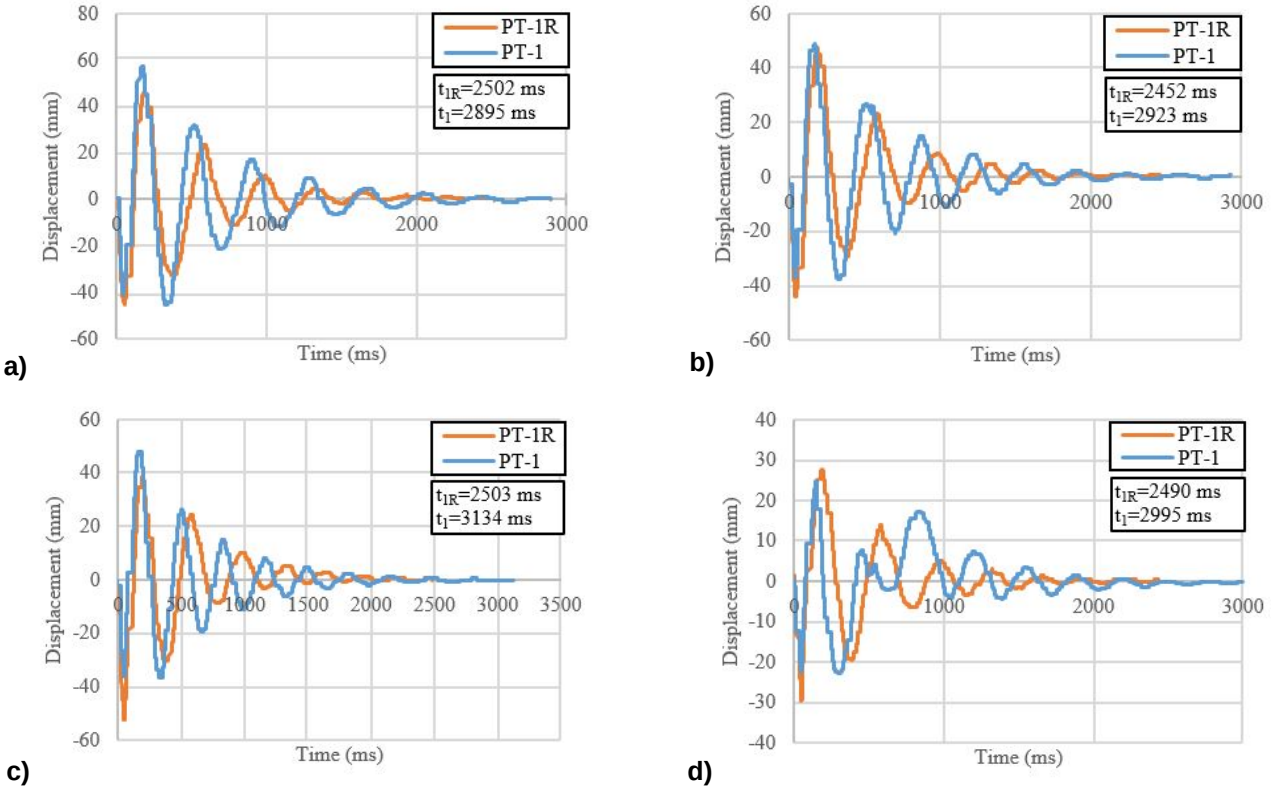

Figure 18. Displacement – Time curves for slabs PT-1 and PT-1R at: (a): ACC0 (b): ACC1 (c): ACC2 (d): ACC3

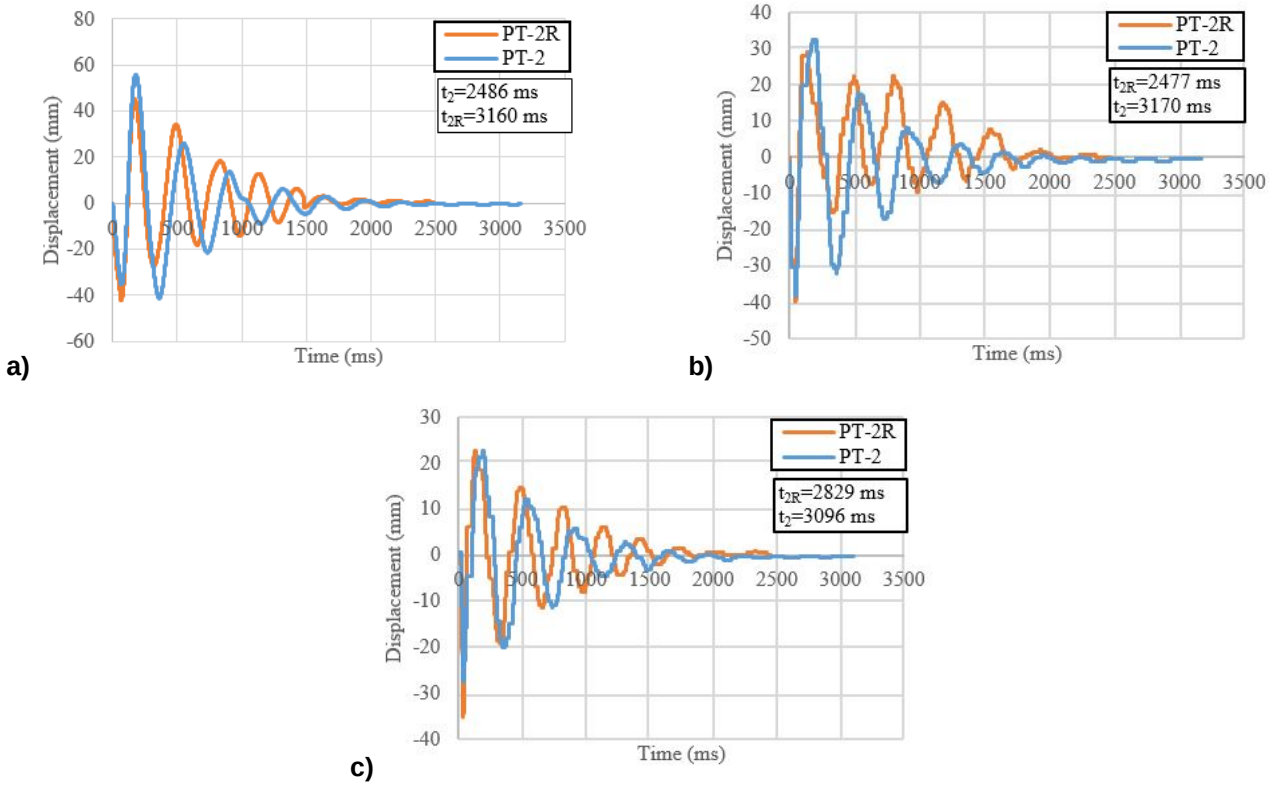

Figure 19: Displacement – Time curves for slabs PT-2 and PT-2R at: (a): ACC0 (b): ACC2 (c): ACC3.

Based on the displacement – time curves illustrated in Figures 18 and 19, vibration analysis was conducted in order to compare the slabs before and after repairing in terms of damping. It can be noted that the vibration time "t" for slab PT-1 was longer than that of slab PT-1R. For example, the vibration time at ACC0 for slabs PT-1 and PT-1R was 2895 and 2502 ms respectively. This trend was realized also for ACC2 where the vibration period was 3134 ms for slab PT-1 compared to 2503 ms for slab PT-1R, although the block falls on its edge and near ACC2 in the case of slab PT-1R. As for the slabs with the edge drop (PT-2 and PT-2R),

ACC0 recorded a vibration time of 3160 ms for slab PT-2 while for slab PT-2R the time was 2486 ms. The trend was the same for the remaining accelerometers (ACC2 and ACC3). This may be due to better damping for the repaired slabs compared to the original ones.

In order to find the damping ratio for each slab, the maximum displacement for each cycle from the displacement – time curves shown in Figures 18 and 19 was plotted and the exponential trend curve passing through these points were presented. This trend curve is called the decaying curve and has the formula $y = Ae^{-w_n \zeta t}$, where y is the displacement, A is a constant, w_n is the natural frequency and is presented by 2Л/T_n, where T_n is the period of vibration, ζ is the damping ratio, and t is the time [23]. Two displacement – time curves (ACC0 and ACC2) were considered for both slabs PT-1 and PT-1R in order to find the damping ratio (Figure 20). Based on the derived exponential functions, the damping coefficient for slab PT-1 at ACC0 is 0.093, whereas for slab PT-1R it is 0.131. The same trend was realized at ACC2, where the value of damping ratio coefficient for slab PT-1 was 0.08 and for PT-1R was 0.11 (Figure 22). Regarding the edge drop case, the time – displacement curves (ACC0 and ACC3) for slabs PT-2 and PT-2R were analyzed (Figure 21). The damping ratio for slab PT-2 at ACC0 was 0.097 whereas for slab PT-2R it was 0.11. As for ACC3, damping ratio values were 0.082 for slab PT-2 and 0.093 for slab PT-2R (Figure 23). This difference in both cases (central and free-edge drop) may be due to varying boundary conditions; since the supports may have been damaged after the first impact. In addition, the original concrete slab parts near the supports were not repaired or replaced causing a difference in the mechanical properties in these zones.

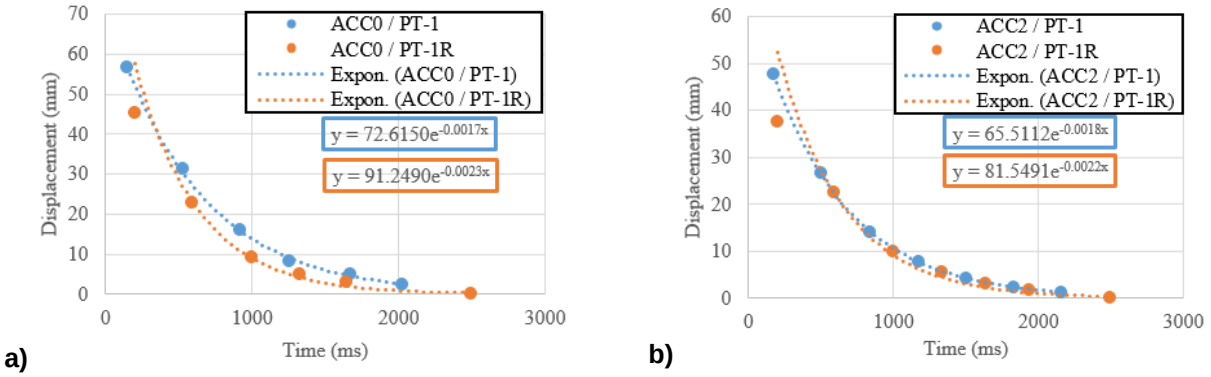

a) b)

Figure 20. Decaying functions for PT-1 and PT-1R at the following accelerometers: (a): ACC0 (b): ACC2

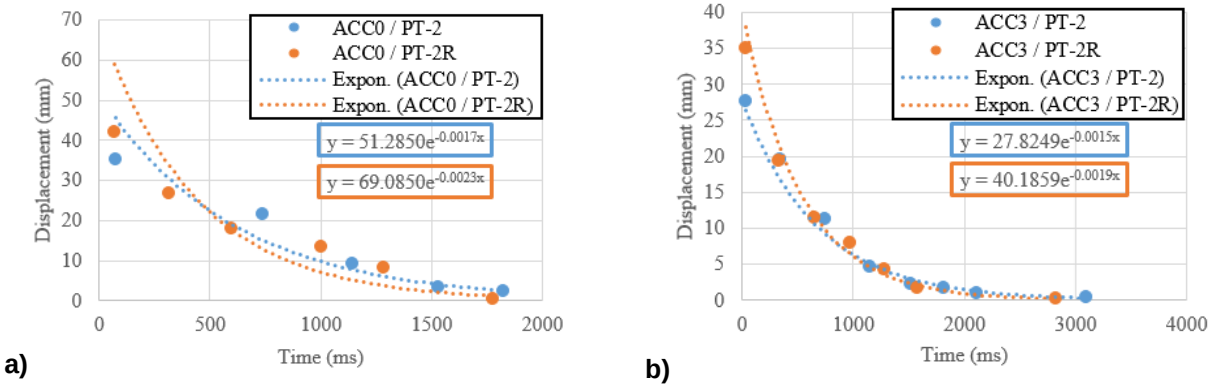

a) b)

Figure 21. Decaying functions for PT-2 and PT-2R at the following accelerometers: (a): ACC0 (b): ACC3

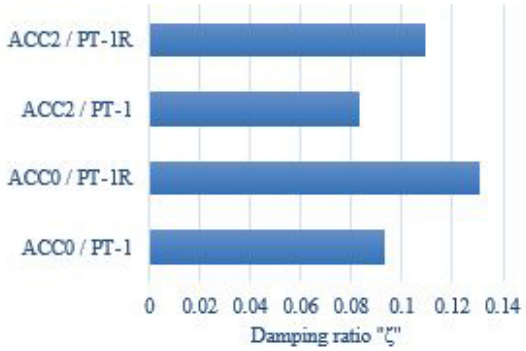

Figure 22. Damping ratio for slabs PT-1 and PT-1R

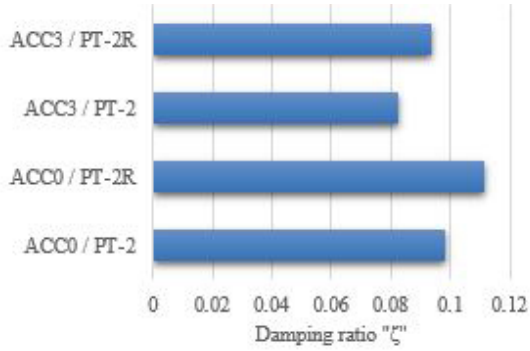

Figure 23. Damping ratio for slabs PT-2 and PT-2R

3.3. Damage Analysis

Table 4 summarizes the damage analysis results. Both slabs PT-1 and PT-2 failed under punching shear mode. This can be shown in Figures 24 and 25. These figures show the distribution of cracks prior to the replacement of concrete parts for both cases (2 m×3 m for central drop case and 4.8 m×3 m for edge drop case). According to these Figures, a spalling phenomenon (Hatched in blue) was observed in both cases. The total spalled zone in tension was 0.82 m^2 for slab PT-1, whereas this area increased to reach 1.1 m^2 for slab PT-2. In addition, crushing of concrete occurred at the top face due to excessive compressive stresses, where the area of crushed concrete was 0.42 m^2 for slab PT-1 and 0.73 m^2 for slab PT-2. This agrees with the previous punching shear analysis carried out (Table 2) where the impact caused the slab to fail under punching shear. Moreover, the damage that occurred for the PT slab subjected to edge impact (PT-2) was more severe than the damage that occurred for the PT slab subjected to central impact (PT-1).

Moreover, slabs PT-1R and PT-2R that were repaired using shear reinforcement had a different crack pattern. Results showed that the damage is changed from punching shear to flexural damage (Figure 25). Slab PT-1R experienced a tiny spalling zone due to the tilting of the block during impact where it fell at its edge as was illustrated in Figures 24b and 24d. As for slab PT-2R, there were no spalling zones as shown in Figure 25. Besides, a distribution for flexural (hairy cracks) was observed for both slabs. These cracks reflect the effect of the concentrated pressure on both slabs from the falling block.

Table 4. Damaged zone areas for tested slabs.

Slab	Crack pattern	Spalling area at tension (m^2)	Spalling area at compression (m^2)
PT-1	Punching shear	0.82	0.42
PT-1R	Flexural	0.01	0.04
PT-2	Punching shear	1.1	0.73
PT-2R	Flexural	0	0

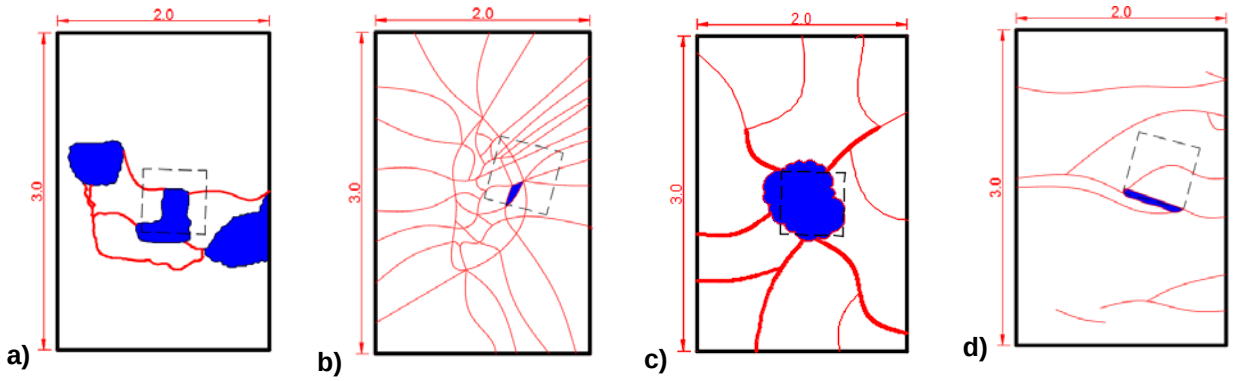

Figure 24. Structural damage (m)
(a): Bottom damage for PT-1 (b): Bottom damage for PT-1R
(c): Top damage for PT-1 (d): Top damage for PT-1R

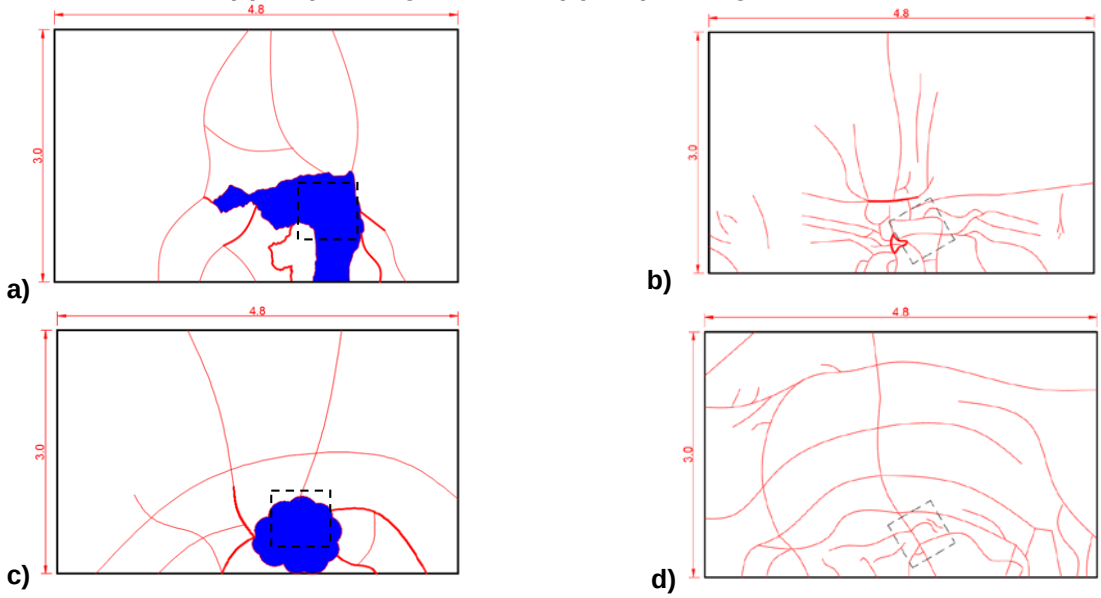

Figure 25. Structural damage (m)
(a): Bottom damage for PT-2 (b): Bottom damage for PT-2R
(c): Top damage for PT-2 (d): Top damage for PT-2R

4. Conclusion

The following conclusions can be made:

1. The position and angle of the falling block have a great effect on the value of impact load acting on PT slabs. Slabs PT-1R and PT-2R, where the falling object landed on its edge, experienced 44 % and 71 % higher impact load than slabs PT-1 and PT-2 respectively, where the falling object landed on its flat surface.

2. Using shear reinforcement helped in enhancing the punching shear capacity for PT slabs when subjected to impact loads. The punching shear resistance was increased by 123% for slabs PT-1 and PT-1R (central drop case), and by 146 % for slabs PT-2 and PT-2R (edge drop case). This improvement was better for edge drop case than central drop case.

3. The normal stress capacity of the repaired slabs was enough to prevent flexural failure. This was proved by showing that both top fibre stresses in compression and bottom rebar stresses in tension were below the ultimate limit specified by the ACI code. The top fiber stress reached 75 % of the code limit for slab PT-1R and 85 % for slab PT-2R. As for the bottom rebar stress, rebars in slab PT-1R reached 63 % of the limit yield strength while in slab PT-2R they reached 91 % of the yield strength. It was concluded that both top and bottom stresses were higher for the edge drop case (PT-2R) than the central drop case (PT-1R) due to the higher strain resulted from the drop upon the free edge.

4. In terms of displacement, the repaired slabs showed a better performance than the original slabs for both central and edge drop case. This was shown in terms of the “Impact force to maximum displacement” (F/D) ratio, where the repaired slabs (PT-1R and PT-2R) had a higher ratio than the original slabs (PT-1 and PT-2). This means that repaired slabs dragged higher forces to cause the same amount of displacement as the original slabs.

5. The repaired slabs (PT-1R and PT-2R) showed to have a higher damping ratio ζ than the original slabs (PT-1 and PT-2). This may be due to the damage occurred for the non-replaced parts near supports; which cause the slabs to dampen in a higher ratio.

6. The crack pattern for PT slabs subjected to impact load is punching shear, where a spalling of concrete occurred at the impact point. Slab PT-2 had a more spalled area in tension and compression than slab PT-1. Using shear reinforcement as a repair technique helped in changing the crack pattern from punching shear to flexure (similar to the effect of concentrated load on slab) for both slabs PT-1R and PT-2R. This helps in preventing brittle failure; since the flexural failure, if happened, is usually designed to be ductile.

7. The results of this investigation suggest that further research is necessary. These include studying the effect of the falling angle and position of the block on the impact resistance of post-tensioned slabs.

References

1. Choi, J.H., Choi, S.J., Kim, J.H.J., Hong, K.N. Evaluation of blast resistance and failure behavior of prestressed concrete under blast loading. Construction and Building Materials. 2018. 173. Pp. 550–572. DOI:10.1016/j.conbuildmat.2018.04.047. URL: https://doi.org/10.1016/j.conbuildmat.2018.04.047.
2. Temsah, Y., Jahami, A., Khatib, J., Sonebi, M. Numerical analysis of a reinforced concrete beam under blast loading. MATEC Web of Conferences. 2018. 149. Pp. 1–5. DOI:10.1051/matecconf/201714902063.
3. Temsah, Y., Jahami, A., Khatib, J., Sonebi, M. Numerical Derivation of Iso-Damaged Curve for a Reinforced Concrete Beam Subjected to Blast Loading. MATEC Web of Conferences. 2018. 149. Pp. 1–5. DOI:10.1051/matecconf/201714902016.
4. Zhang, D., Yao, S.J., Lu, F., Chen, X.G., Lin, G., Wang, W., Lin, Y. Experimental study on scaling of RC beams under close-in blast loading. Engineering Failure Analysis. 2013. 33. Pp. 497–504. DOI:10.1016/j.engfailanal.2013.06.020.
5. Mougin, J.P., Perrotin, P., Mommessin, M., Tonnelo, J., Agbossou, A. Rock fall impact on reinforced concrete slab: An experimental approach. International Journal of Impact Engineering. 2005. 31(2). Pp. 169–183. DOI:10.1016/j.ijimpeng.2003.11.005.
6. Jahami, A., Temsah, Y., Baalbaki, O., Darwiche, M., Al-Rawi, Y., Al-Ilani, M., Chaaban, S. Effect of Successive Impact Loads From a Drop Weight on a Reinforced Concrete Flat Slab. MATEC Web of Conferences. 2019. 281. Pp. 02003. DOI:10.1051/matecconf/201928102003.
7. Iqbal, M.A., Kumar, V., Mittal, A.K. Experimental and numerical studies on the drop impact resistance of prestressed concrete plates. International Journal of Impact Engineering. 2019. 123. Pp. 98–117. DOI:10.1016/j.ijimpeng.2018.09.013. URL: https://doi.org/10.1016/j.ijimpeng.2018.09.013.
8. Al Rawi, Y., Timsah, Y., Ghanem, H., Jahami, A., Elani, M. The effect of impact loads on prestressed concrete slabs. The Second European and Mediterranean Structural Engineering and Construction Conference. (July)2018.
9. Kumar, V., Iqbal, M.A., Mittal, A.K. Energy absorption capacity of prestressed and reinforced concrete slabs subjected to multiple impacts. Procedia Structural Integrity. 2017. 6. Pp. 11–18. DOI:10.1016/j.prostr.2017.11.003. URL: https://doi.org/10.1016/j.prostr.2017.11.003.
10. Almusallam, T., Al-Salloum, Y., Alsayed, S., Iqbal, R., Abbas, H. Effect of CFRP strengthening on the response of RC slabs to hard projectile impact. Nuclear Engineering and Design. 2015. 286. Pp. 211–226. DOI:10.1016/j.nucengdes.2015.02.017.
11. Kong, X., Qi, X., Gu, Y., Lawan, I.A., Qu, Y. Numerical evaluation of blast resistance of RC slab strengthened with AFRP. Construction and Building Materials. 2018. 178. Pp. 244–253. DOI:10.1016/j.conbuildmat.2018.05.081. URL: https://doi.org/10.1016/j.conbuildmat.2018.05.081.
12. Ali, T., Yehia, S. Study on Strengthening of RC Slabs with Different Innovative Techniques. Open Journal of Civil Engineering. 2016. 06(04). Pp. 516–525. DOI:10.4236/ojce.2016.64044.

13. Radnić, J., Matešan, D., Grgić, N., Baloević, G. Impact testing of RC slabs strengthened with CFRP strips. Composite Structures. 2015. 121. Pp. 90–103. DOI:10.1016/j.compstruct.2014.10.033.
14. Jahami, A., Temsah, Y., Khatib, J., Sonebi, M. Numerical study for the effect of carbon fiber reinforced. Symposium on Concrete Modelling (CONMOD2018). (August)Delft, Netherlands, 2018. Pp. 259–267.
15. Hao, Y., Hao, H., Chen, G. Experimental tests of steel fibre reinforced concrete beams under drop-weight impacts. Key Engineering Materials. 2015. 626(August). Pp. 311–316. DOI:10.4028/www.scientific.net/KEM.626.311.
16. Harajli, M.H., Maalouf, D., Khatib, H. Effect of fibers on the punching shear strength of slab-column connections. Cement and Concrete Composites. 1995. 17(2). Pp. 161–170. DOI:10.1016/0958-9465(94)00031-S.
17. Mostafaei, H., Vecchio, F.J., Gauvreau, P., Semelawy, M. Punching shear behavior of externally prestressed concrete slabs. Journal of Structural Engineering. 2011. 137(1). Pp. 100–108. DOI:10.1061/(ASCE)ST.1943-541X.0000283.
18. Abir, J., Longo, S., Morantz, P., Shore, P. Optimized estimator for real-time dynamic displacement measurement using accelerometers. Mechatronics. 2016. 39. Pp. 1–11. DOI:10.1016/j.mechatronics.2016.07.003.
19. Yang, J., Li, J.B., Lin, G. A simple approach to integration of acceleration data for dynamic soil-structure interaction analysis. Soil Dynamics and Earthquake Engineering. 2006. 26(8). Pp. 725–734. DOI:10.1016/j.soildyn.2005.12.011.
20. Automated Test and Automated Measurement Systems - National Instruments, 2019. URL https://www.ni.com/en-lb.html [accessed 22 August 2019].
21. Building Code Requirements For Structural Concrete (ACI 318-14). Farmington Hills, Michigan: American Concrete Institute, ACI. 2014.
22. MC90, CEB-FIP Model Code 1993, Design Code, 6th edition, Thomas Telford, Lausanne, Switzerland, 1993.
23. Chopra, Anil K. Dynamics Of Structures. 4th edn. 2009.

Contacts:

Ali Jahami, +96171859962; ahjahamy@hotmail.com
Yehya Temsah, +9613723790; ytemsah@bau.edu.lb
Jamal Khatib, +96170382861; j.m.khatib@wlv.ac.uk
Ossama Baalbaki, +9613348851; obaalbaki@bau.edu.lb
Mohamad Darwiche, +96176602500; m.darwich@bau.edu.lb
Sandy Chaaban, +9613627858; s.chaaban@bau.edu.lb